Corrosion Science 55 (2012) 153–163

Contents lists available at SciVerse ScienceDirect

Corrosion Science

journal homepage: www.elsevier.com/locate/corsci

Influence of Al and Y on the ignition and flammability of Mg alloys

Arvind Prasad, Zhiming Shi, Andrej Atrens *

The University of Queensland, Materials Division, Brisbane 4072, Australia

ARTICLE INFO

Article history:
Received 9 July 2011
Accepted 11 October 2011
Available online 20 October 2011

Keywords:
A. Magnesium
C. Oxidation

ABSTRACT

The influence of alloying on the ignition and flammability was studied. One end of a cylindrical specimen was exposed to a free diffusion flame. Ignition required at least partial melting. Burning extinguished once the flame was withdrawn. Specimen tips of pure Mg, AZ61, and AZ91 ignited upon prolonged flame exposure. There was smouldering and delayed ignition for Mg-1Y. There was no ignition for Mg-5Y specimen tips, attributed to a protective surface oxide containing Y. The results indicate that (i) vigorous burning requires a continued supply of Mg vapour, and (ii) a critical alloy concentration is required to change ignition behaviour.

1. Introduction

Magnesium (Mg) alloys have a low density and a good strength to weight ratio. However, Mg is inherently reactive so that Mg alloys have moderate corrosion resistance [1–4]. Oxidation is also an issue, so that the melting Mg alloys typically needs a cover gas [5]. Research has been carried out to identify alloying elements, which would render Mg alloys ignition-proof without the need for a cover gas or a flux. Chen et al. [6] and Jin-song et al. [7] found that AZ91D and ZM5 containing 0.1 wt%RE (rare earth elements) showed a significant increase in the ignition temperature of ~200 °C, attributed to surface segregation and a protective surface oxide: RE_2O_3. Sakamoto et al. [8] also found a 200 °C increase in the ignition temperature for an alloy containing 5 wt%Ca. Xiaoqin et al. [9,10] found that Mg alloys containing 0.3 wt%Be, or 0.3 wt%Be + 1 wt%RE, could be melted and poured without a flux or cover gas, attributed to the formation of a protective layer of BeO.

Other studies identified the ignition temperature as the temperature at which the temperature showed a sudden increase on heating a specimen in a furnace, due to the onset of burning. Fassell et al. [11] found that alloying reduced the ignition temperature for the alloying elements they studied (17 binary and 4 ternary alloys), except for Ca. Defining melting point as the liquidus of the alloy, they showed that ignition took place either above or below the melting point of the alloy. Li et al. [12] and Huang et al. [13] found that the ignition temperature of AZ91 increased by 60–80 °C, attributed to CeO formation within the porous surface MgO, thereby inhibiting further oxidation. Similarly, Lin et al. [14,15] found that increasing concentrations of Ce (0–1 wt%) increased the ignition temperature of rapidly solidified AM50 by up to 60 °C. In contrast, there was an increase in ignition temperature at low Ce concentrations (0.15 wt%) for normally solidified AM50 and AZ91, but the ignition temperature decreased on increasing the Ce concentration to 1 wt%. This difference in the influence of Ce was attributed to less Ce available for protective Ce-oxide formation in normally solidified specimens, where $Al_{11}Ce_3$ intermetallics were formed. $Al_{11}Ce_3$ formation was suppressed in rapidly solidified specimens. Similarly, the ignition temperature of AZ91D powders increased [14,15] for Y concentrations up to 0.2 wt%, followed by a decrease. This was similarly explained in terms of Al_2Y formation that depleted the Y available for protective Y-oxide formation. In contrast, Fan et al. [16] found that Ce concentrations up to 13 wt% in Mg resulted in no difference in ignition temperature, whereas Y (either by itself or in combination with Ce) caused a significant increase in ignition temperature (up to 150 °C), attributed to the formation of a Y containing oxide.

Shih et al. [17], by measuring the enthalpy release during heating, found that that the ignition temperature decreased with Zn content for the AZ series alloys, and increased with Ca concentration for Mg–Ca alloys. The lowering of the ignition temperature for the AZ series was attributed to the melting of phases with low melting temperature. You et al. [18] found that Al and Y increased significantly the ignition temperature of Mg-2 wt%Ca, attributed to changes of the surface oxide. Likewise, Choi et al. [19] found that increasing Ca content, in the range 0.3–5 wt%, increased the ignition temperature of AZ91 and that Be, in the range 0.002–0.005 wt.%, further increased the ignition resistance. Huang et al. [20] produced similar results for pure Mg containing Ca and Be.

Ignition and flammability are different quantities although sometimes they are used interchangeably. Both are a result of oxidation. However, although there may be ignition, flames require a sustained reaction rate. Eyring and Zwolinski [21] indicated that heat conduction away from the oxide-metal interface can prevent ignition. During the melting and pouring of Mg alloys, there is a

* Corresponding author. Tel.: +61 7 3365 3748.
E-mail address: Andrejs.Atrens@uq.edu.au (A. Atrens).

0010-938X/$ - see front matter © 2011 Elsevier Ltd. All rights reserved.
doi:10.1016/j.corsci.2011.10.014

significant amount of Mg vapour. This allows high rates of combustion, and thus ignition is often followed by burning with flames. Similarly, Mg specimens heated in a furnace can burn readily, because of the availability of Mg vapour. In contrast, there are a number of possibilities for a Mg alloy subjected to a flame. There may be no ignition if there is insufficient heat input. If there is ignition, burning may extinguish if sufficient heat is extracted from the Mg specimen.

Our prior research [22] used a simple furnace test to explore the ignition of Mg alloys. It was concluded that flame tests appear to allow study of the behaviour of a Mg alloy under a direct flame. Flame tests thus appear to be a good approach to study the behaviour Mg alloys in an aircraft or auto fire accident.

The current research aims to study the influence of Al and Y in Mg alloys on ignition and flammability for Mg alloy specimens subjected directly to a flame. The research is aligned with auto and aerospace applications, where a solid component can potentially be exposed to a direct source of heat, such as an in-flight fire or in a post-crash fire.

2. Experimental procedure

2.1. Specimen materials

Five Mg alloys were studied: High Purity (HP) Mg, AZ61, AZ91, Mg-1Y and Mg-5Y. Table 1 presents the composition of the alloys, determined by ICP-AES by Spectrometer Services, Coburg, Vic. AZ61 and AZ91 were produced by melting HP Mg at 690 °C, and adding appropriate amounts of Al (99.96 wt% purity) and Zn (99.995 wt% purity). Mg-1Y and Mg-5Y were produced by adding appropriate amounts of pure Y (99.8 wt%) to molten HP Mg at 730 °C. A SF_6(1%)–CO_2(50%) mixture pre-mixed with CO_2 was used as a cover gas during the entire melting sequence. Refrigerant gas R134a was used to envelope the liquid metal during pouring into the moulds, which were pre-flushed with the same gas.

Round specimens 8 mm and 20 mm in diameter were produced by pouring each melt into two-part steel moulds aligned with dowel pins, at 710 °C to ensure fluidity during casting. The inside of the moulds was coated with BN to minimise Fe pickup by the molten alloy from the steel mould. The two parts of the mould were clamped with C-clamps during pouring to minimise flash formation. The flash was removed prior to the flame tests. All the specimens were machined to a nominal length of 200 mm. Some of the AZ61 and AZ91 specimens were machined to a diameter of 16 mm.

2.2. Flame tests

Fig. 1 shows a schematic of a flame test. One end of the horizontal cylindrical specimen was exposed to the flame from a liquified petroleum gas (LPG) nozzle. This flame is designated herein as a LPG flame. Atmospheric air was post-mixed freely with the fuel. The fuel was supplied from a commercial LPG bottle. Two K-type thermocouples, of 1 mm diameter, were embedded in the specimen as shown in Fig. 1(a), to measure the temperature, T. A K-type thermocouple was also placed in the flame to monitor the flame temperature. The thermocouple data were displayed and recorded using a National Instruments data acquisition system (NI USB 9162).

Table 1
Chemical composition (wt%) of the alloys.

Alloy	Al	Zn	Y	Fe	Mn	Mg
HP Mg	0.007	–	–	0.002	0.04	Bal.
AZ61	6.2	0.2	–	0.002	0.3	Bal.
AZ91	8.7	0.7	–	0.003	0.2	Bal.
Mg-1Y	0.06	–	1.3	0.004	0.05	Bal.
Mg-5Y	0.005	0.01	6.3	0.009	0.05	Bal.

The LPG flame exhibited a blue colour, which indicated that the combustion of the fuel was complete. This was also confirmed by the lack of soot deposits on the specimens after the tests. The LPG flame exhibited an approximately circular cross-section of 25 mm diameter. The LPG flame coverage of the specimen tip was adjusted to 20 mm, so that there was no direct contact between the LPG flame and the TC_1 thermocouple.

Using the experimental arrangement illustrated in Fig. 1, with the gas throttle at full, two sets of tests were performed for each alloy and geometry. These are designated as a (i) T-test and (ii) melting test. The T-tests were used to identify the lower temperature limit, if any, above which melting or ignition occurred, and to study the relationship between ignition and melting. The specimen was exposed to the LPG flame and the TC_1 thermocouple temperature was tracked until it reached a pre-defined target temperature, at which time the LPG flame was extinguished. The target temperatures were chosen to be lower than the equilibrium alloy solidus or the melting temperature of HP Mg. For a melting test, the LPG flame was extinguished following initial melting of the specimen tip, either immediately, or, after a period of time.

Blob flammability tests were carried out using small discs of HP Mg as shown in Fig. 1(d) to investigate the combustion behaviour of detached blobs. A thin disc (20 mm diameter and 5 mm thick) simulated a blob detached from a specimen tip during a flame test. The disc was exposed to a direct LPG flame until it ignited, at which time the LPG flame was extinguished.

3. Results

3.1. Flame temperature

The LPG flame temperature was measured, as shown in Fig. 1(c), using four thermocouples at 25, 50, 75 and 100 mm distance from the mouth of the nozzle. The gas flow was at quarter, half and full throttle. Fig. 2(a) shows typical temperatures at full throttle as measured by the four thermocouples. Each thermocouple indicated that the LPG flame temperature quickly attained steady state. Temperatures at 50 and 75 mm were higher than at 25 or 100 mm. The LPG flame edge was sharp up to 75 mm, whereas, the LPG flame edge became blurred near 100 mm, particularly for half and quarter throttle. Thus the LPG flame was kept constant in all tests by performing all flame tests with the nozzle mouth to specimen distance at 50 mm, with full gas throttle. This arrangement is shown in Fig. 1(b). Fig. 2(b) illustrates typical LPG flame temperatures for repeat temperature measurements. The variability was less than 20 °C. These LPG flame temperatures were not corrected for radiation effects since the flame characteristics were kept constant for each experiment.

3.2. Specimen tip temperature

Fig. 3(a) shows a typical thermal profile from a T-test using a 20 mm diameter HP Mg specimen. The pre-assigned T_1 temperature (corresponding to the thermocouple TC_1) had been set to 575 °C. The LPG flame caused an increase in temperatures T_1 and T_2. T_1 was beginning to plateau towards the end of the exposure to the LPG flame, whereas T_2 had a shallow gradient till the end of the LPG flame exposure. After LPG flame withdrawal, T_1 decreased immediately, whereas T_2 continued to increase for some time before decreasing. This continued increase in T_2 was because heat continued to be conducted along the specimen from the flame-exposed end to the cooler unexposed end.

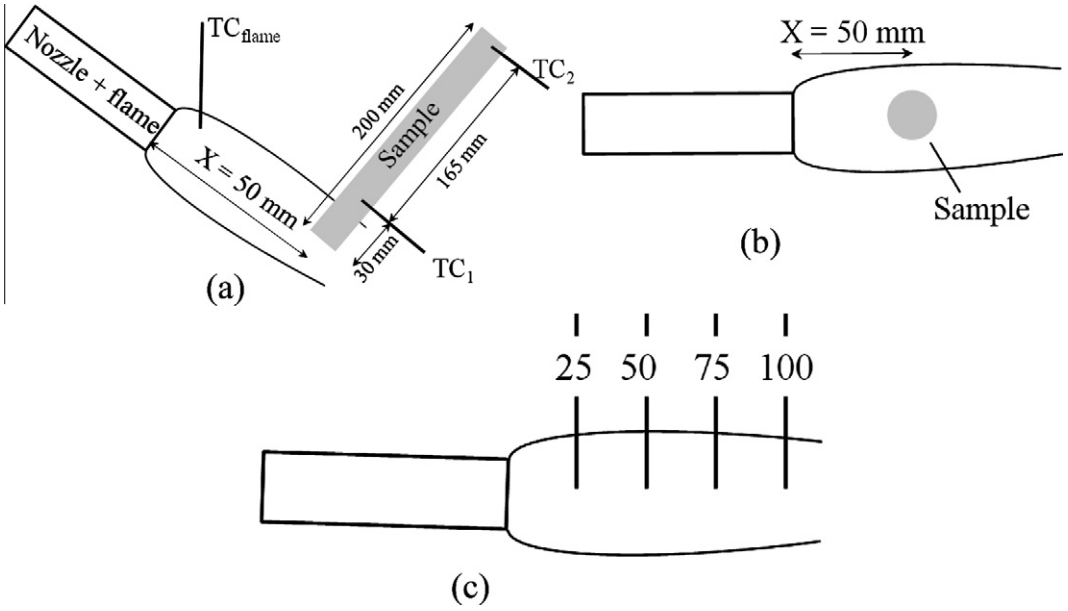

Fig. 1a–c. Schematic of the experimental arrangement showing (a) top view of the nozzle, flame, specimen and embedded thermocouples (TC1 and TC2); (b) front-view of a 20 mm specimen exposed to the flame; and (c) top view of the thermocouple positions (in mm from the end of the nozzle) for the measurement of flame temperatures.

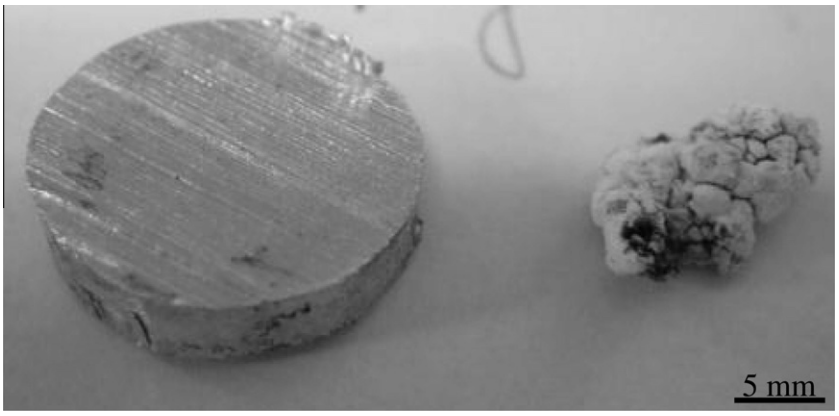

Fig. 1d. Blob flammability tests were carried out using small discs of HP Mg as shown to investigate the self-sustaining combustion behaviour of detached blobs. A thin disc (20 mm in diameter and 5 mm thick), simulating a blob detached from a specimen tip during a flame test, was exposed to a direct LPG flame until it ignited, at which point the LPG flame was removed. Also shown is the oxide mass after burning of the blob.

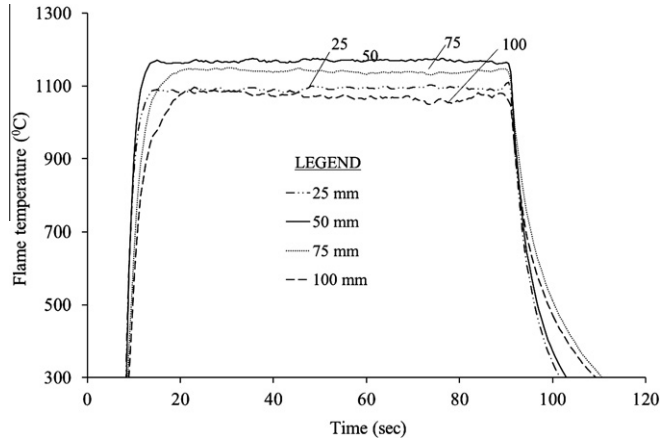

Fig. 2a. Flame temperature as measured by thermocouples in the LPG flame, positioned as shown in Fig. 1(c).

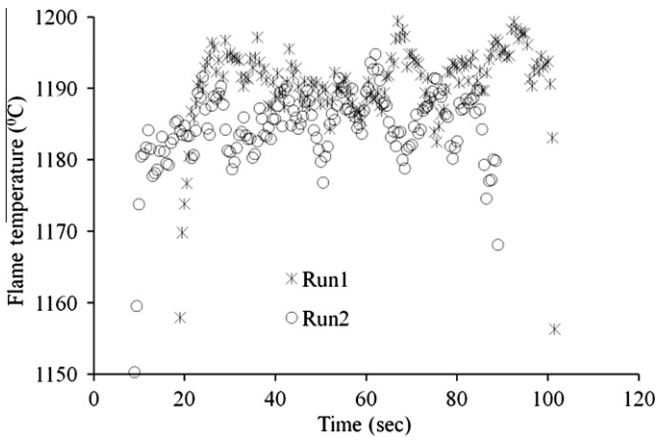

Fig. 2b. Reproducibility and stability of the LPG flame temperature as measured by a thermocouple in the flame 50 mm from the nozzle.

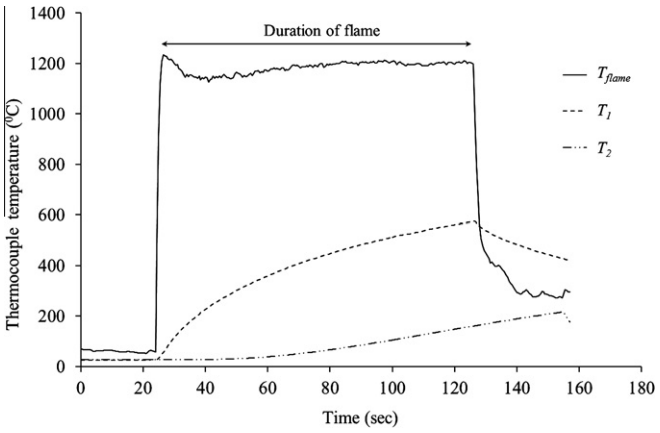

Fig. 3a. Typical thermal profile for a *T*-test using a 20 mm HP Mg specimen.

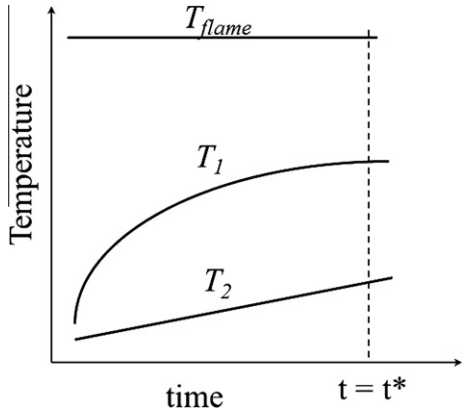

Fig. 3b. Schematic of Fig. 3(a) illustrates the quasi-steady-state approximation for estimating the specimen tip temperature. The specimen was assumed to be at thermal steady state when *t* approached *t**.

A melting test showed a similar temperature profile. The significant difference was a delay in the drop in T_1 temperature following melting and ignition. Fig. 4 shows a typical temperature profile for AZ61specimens, 20 mm and 8 mm in diameter. The LPG flame was withdrawn when melting initiated. This coincided with the peak TC_1 thermocouple temperature. For both specimen diameters, the peak temperature recorded by the TC_1 thermocouple was lower than the freezing range of AZ61 even when the specimen exhibited melting at the tip. This is attributed to (i) transient heat conduction through the specimen, and (ii) convective heat loss from the specimen to the surroundings. Thus, the T_1 temperatures for both 20 mm and 8 mm specimens showed temperatures lower than the melting temperature at the tip. Furthermore, for the same tip temperature, the thinner (8 mm) diameter specimen showed a lower T_1 temperature, attributed to larger convective heat loss for the smaller diameter specimen. In contrast to Fig. 3(a), the TC_2 thermocouple temperature in Fig. 4 did not rise above 30 °C for AZ61, and similar observations were made for AZ91.

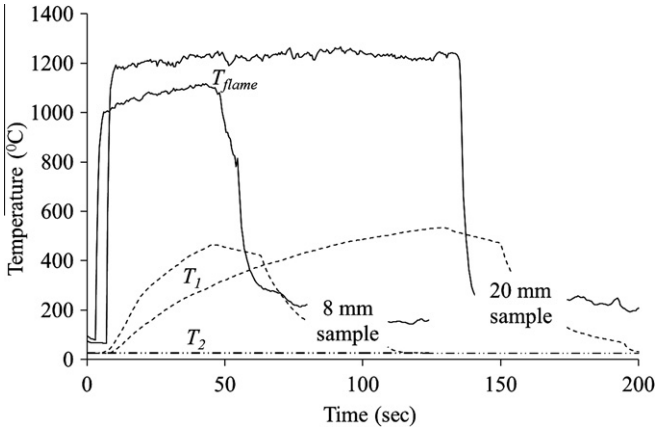

Fig. 4. Typical thermal profiles for a melting test using 20 mm and 8 mm AZ61 specimens.

Fig. 4 shows that the experimental time to melting for the 8 mm specimen was shorter than for the 20 mm specimen, indicating faster heating rates for the smaller diameter specimen. The TC_1 thermocouple temperature profiles for the two specimens show a slight recalescence following the peak temperature (at which time the LPG flame was withdrawn) with a subsequent sharp drop in temperature, similar to the temperature drop for a *T*-test (Fig. 3(a)). The latent heat release during melting resulted in the recalescence.

There were similar temperature profiles for both tests for all alloys of all diameters. Thus only typical thermal profiles are reported.

3.3. HP Mg

Table 2 summarises the tests performed with HP Mg. These were: one melting test (specimen #1) and *T*-tests (specimens #2–6) with target T_1 temperatures of 580 and 600 °C for 20 mm specimens, and 500, 550 and 580 °C for 8 mm specimens. The target T_1 temperatures for the 8 mm specimens were lower since the difference between the tip temperature and T_1 was greater for the smaller diameter specimen. Table 2 reports the peak temperature measured by thermocouple TC_1, and the experimental observations.

For the 20 mm specimens, there was no specimen tip melting for a T_1 peak temperature of 575 °C, whereas there was specimen tip melting for higher T_1 peak temperatures. This indicated that the T_1 peak temperatures were related to the specimen tip temperatures for these 20 mm specimens. Furthermore, there was no ignition associated with the specimen with no melting at the specimen tip for the T_1 peak temperature of 575 °C. Fig. 5(a) shows the unmelted and unignited tip of the 20 mm HP Mg specimen. At a higher target temperature, following melting at the specimen tip, a small blob detached from the specimen tip. Both the specimen tip and the detached blob burnt vigorously. Fig. 5(b) shows such a HP Mg specimen tip, which had melted and the specimen tip had ignited.

Table 2
Flame test results for HP Mg.

#	Specimen diameter (mm)	Target T_1 temperature (°C)	Peak T_1 temperature (°C)	Observations	
				Melting	Specimen ignition
1	20	–	612	Yes, detached blob	Blob + specimen, vigorous
2	20	600	592	Yes, detached blob	Blob + specimen, vigorous
3	20	580	575	No	No
4	8	580	491	Yes, detached blob	Blob + specimen, vigorous
5	8	550	521	Yes, detached blob	Blob + specimen, vigorous
6	8	500	514	Yes	Yes, non-vigorous

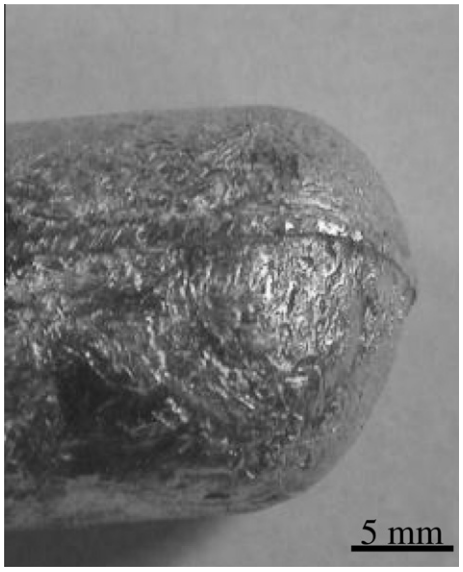

Fig. 5a. Un-melted and un-burnt post-experiment condition for a 20 mm HP Mg specimen tip (specimen #3 in Table 2).

All the 8 mm specimen tips melted and subsequently ignited. The fact that all the 8 mm specimen tips melted indicated that the target T_1 temperatures were set to be above the T_1 temperature corresponding to specimen tip melting.

Following initial melting of the specimen tip, the formation of a molten blob and its detachment was observed to be dependent on the duration of the LPG flame exposure. A blob of molten metal was observed to detach if sufficient melting had taken place. These blobs were observed to either (i) ignite just prior to detachment under the exposure of the LPG flame, or (ii) upon detachment as an unignited blob, the blob would ignite when away from the LPG flame. In either case, the blobs were observed to continue to burn. Fig. 6(a) and (b) shows in sequence the burning of both the specimen tip and the molten blob. The blob continued to burn with flames, whereas the flames of the specimen tip extinguished.

The additional blob flammability tests, carried out using small discs of HP Mg as shown in Fig. 1(d), indicated that the disc ignited and continued to burn with flames, at the end of which only a white residue (presumed to be MgO) remained, also shown in Fig. 1(d). Once ignited, the flames of the disc did not extinguish. The disc continued to burn even though the LPG flame was removed.

Following blob detachment, the specimen tip only ignited if the LPG flame was kept on the specimen tip for some additional time. Such specimen tips, which formed a blob and both the specimen tip, and the blob (detached or attached), burnt vigorously, are designated as "vigorous" in Table 2. If the LPG flame was withdrawn immediately after blob formation, minimal specimen tip ignition took place and this is denoted as "non-vigorous". In general the non-vigorous burning specimen tips had a small amount of melting due to which the molten blob remained attached to the specimen tip. In either case of vigorous burning or non-vigorous burning, the flame of the specimen tip extinguished some time after the LPG flame was withdrawn. Thus, the burning of the detached blob was self-sustaining whereas the flame of the specimen tip extinguishing unless extended heat was provided.

3.4. AZ61

Table 3 presents the results for *T*-tests for AZ61. For 20 mm specimens, there was no melting for T_1 target temperatures up to 550 °C. There was no ignition for any specimen tip that did not melt. Some low target temperatures resulted in some melting of the specimen tip. In these cases the specimens had an attached molten blob, which did not ignite. At higher target temperatures, detached molten blobs were formed. There was specimen tip burning only in these cases. The sequence of melting and subsequent ignition in the AZ61 specimen tips was observed to be the same as for the HP Mg specimen tips. This was case for both specimen diameters.

Table 4 presents the results of the melting tests for AZ61. These show that following melting of the specimen tip, the molten blob either remained attached to the specimen tip or detached, depending upon the extent of LPG flame exposure. Following sufficient melting, the molten blob detached from the specimen tip. The attached molten blob only ignited when there was extended LPG

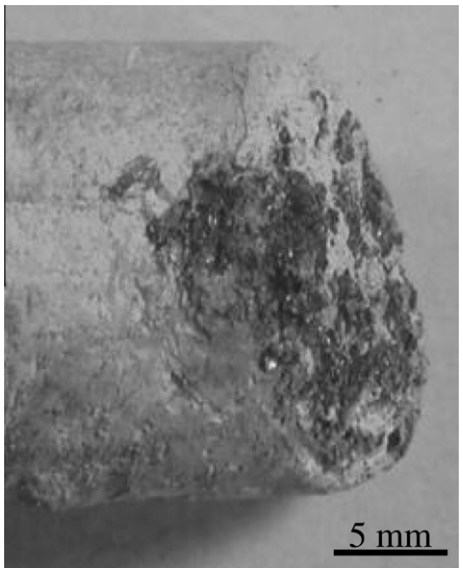

Fig. 5b. Melted and burnt post-experiment condition for a 20 mm HP Mg specimen tip (specimen #2).

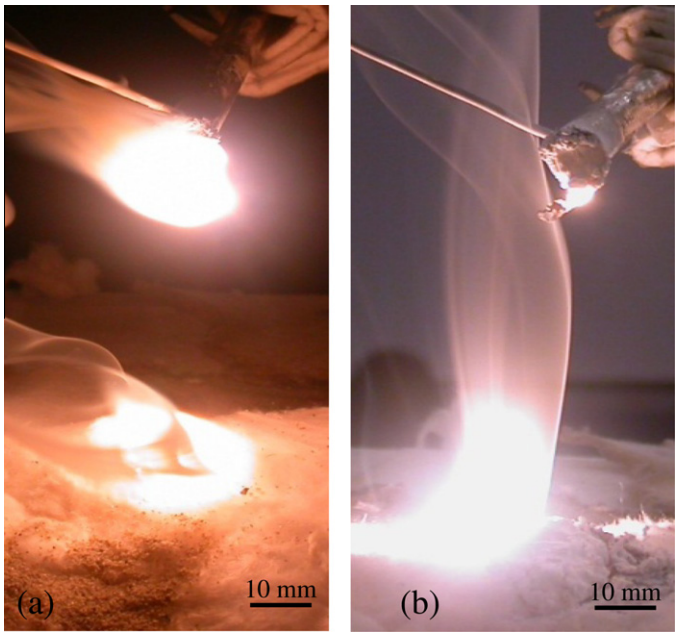

Fig. 6. Image sequence from a flame test using HP Mg. (a) The specimen and the fallen molten blob both ignited and burnt with a flame. (b) The detached blob continued to burn whereas the flame of the specimen tip extinguished.

Table 3
T-test results for AZ61 and AZ91.

#	Alloy, diameter (mm)	Target T_1 temperature (°C)	Peak T_1 temperature (°C)	Observations	
				Melting	Specimen ignition
1	AZ61, 20	475	464	No	No
2	AZ61, 20	475	470	No	No
3	AZ61, 20	475	495	No	No
4	AZ61, 20	500	500	No	No
5	AZ61, 20	500	510	No	No
6	AZ61, 20	525	528	Incipient melting	No
7	AZ61, 20	525	534	No	No
8	AZ61, 20	550	551	No	No
9	AZ61, 20	550	548	Yes, attached blob	No
10	AZ61, 20	575	556	Yes, detached blob	Yes, non-vigorous
11	AZ61, 20	575	558	Yes, detached blob	Yes, vigorous
12	AZ61, 8	425	435	Yes, attached blob	No
13	AZ61, 8	425	441	Incipient melting	No
14	AZ61, 8	450	465	Yes, attached blob	No
15	AZ61, 8	475	480	Yes, attached blob	No
16	AZ91, 20	475	469	No	No
17	AZ91, 20	475	477	No	No
18	AZ91, 20	500	502	No	No
19	AZ91, 20	500	500	No	No
20	AZ91, 20	525	527	Yes, attached blob	Yes, vigorous
21	AZ91, 20	550	556	Yes, attached blob	No
22	AZ91, 20	550	513	Yes	Yes, non-vigorous
23	AZ91, 20	525	509	Yes	Yes, non-vigorous
24	AZ91, 8	400	441	Yes, attached blob	No
25	AZ91, 8	475	569	Yes, detached blob	Yes, vigorous
26	AZ91, 8	475	505	Yes, detached blob	Yes, vigorous

flame exposure (such as specimen #4). The detached unignited molten blob, upon falling out of the LPG flame, always ignited and continued to burn. For specimen tips with a detached molten blob, there was no ignition of the specimen tip when the LPG flame was withdrawn immediately. For those cases where the specimen tips did ignite following melting, the flames of the specimen tips extinguished upon withdrawal of the LPG flame. The ignited detached molten blobs continued to burn in all cases.

Fig. 7 shows the typical sequence of melting followed by ignition for AZ61. During prolonged LPG flame exposure of a 20 mm specimen, the specimen tip initially melted (Fig. 7(a)), multiple ignition kernels formed within the melted tip (Fig. 7(a) and (b)), leading to vigorous localised burning of the molten blob which detached leaving the unignited specimen (Fig. 7(c)). The detached molten blob continued to burn (Fig. 7(c)).

3.5. AZ91

Table 3 also presents the results for *T*-tests for AZ91. These results also indicated that there was no ignition without some melting. Melting of 20 mm specimen tips initiated only for T_1 temperatures at or above 525 °C. Specimen tip ignition subsequent to melting occurred only at higher temperatures.

Table 4 also presents the results of the melting tests for AZ91. These results were similar to those for HP Mg and AZ61. A small amount of melting followed by immediate withdrawal of the LPG flame did not result in vigorous burning of the specimen tip. Vigorous burning was always a result of sustained LPG flame exposure and the formation of a detached blob. In particular, specimen #9 was exposed to the LPG flame for a prolonged time (>120 s), which resulted in vigorous burning of the specimen tip. The sequence of melting and ignition as depicted in Fig. 7 for AZ61specimen tips was also observed for AZ91.

Fig. 8 presents images to illustrate the role of flame exposure in the melting and ignition for AZ61 and AZ91 specimen tips. Fig. 8(a) shows a molten attached unignited blob for an 8 mm AZ61specimen. Fig. 8(b) shows a molten but unignited 20 mm AZ91 specimen tip. Fig. 8(c) shows a burnt 20 mm AZ91 specimen tip.

In summary, the ignition and flammability characteristics were identical for all diameters of the three alloys: HP Mg, AZ61 and

Table 4
Melting test results for AZ61 and AZ91.

#	Alloy, diameter (mm)	Peak T_1 temperature (°C)	Observations	
			Melting	Specimen ignition
1	AZ61, 20	565	Yes, detached blob	Blob ignition only, no specimen ignition
2	AZ61, 16	535	Yes	Some ignition, non-vigorous
3	AZ61, 16	575	Yes	Some ignition, non-vigorous
4	AZ61, 16	565	Yes, detached blob	Specimen and blob ignition, vigorous
5	AZ61, 8	540	Yes, detached blob	Blob ignition only, no specimen ignition
6	AZ61, 8	494	Yes, detached blob	Blob ignition only, no specimen ignition
7	AZ91, 20	498	Yes, attached blob	Some ignition, non-vigorous
8	AZ91, 20	502	Yes, detached blob	Some ignition, non-vigorous
9	AZ91, 20	557	Yes, detached blob	Very long exposure; self-sustained ignition
10	AZ91, 16	484	Yes	Some ignition, non-vigorous
11	AZ91, 16	533	Yes	Some ignition, non-vigorous
12	AZ91, 16	491	Yes, detached blob	Specimen and blob ignition, vigorous
13	AZ91, 8	406	Yes, no blob	Some ignition, non-vigorous
14	AZ91, 8	493	Yes, detached blob	Specimen and blob ignition, vigorous
15	AZ91, 8	501	Yes, detached blob	Specimen and blob ignition, vigorous

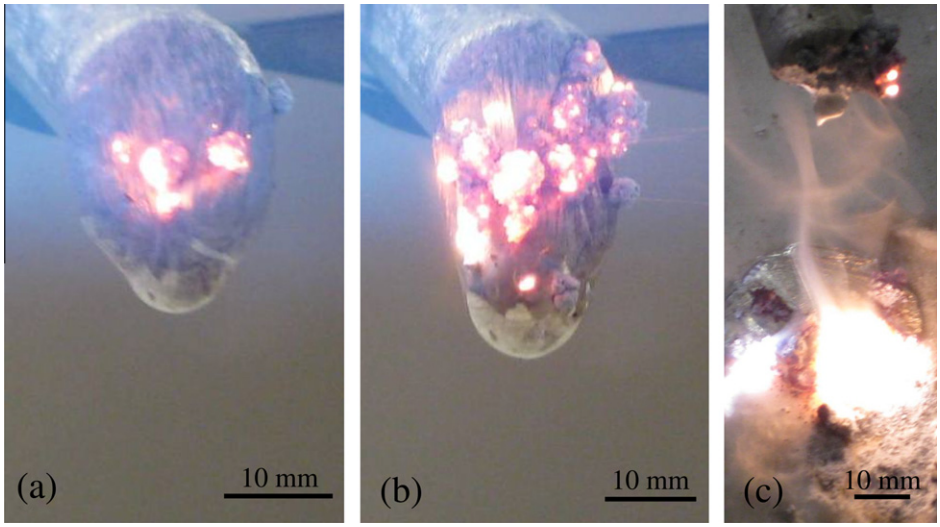

Fig. 7. Flame melting test using AZ61. (a) The specimen tip exposed to the flame melted; (b) followed by ignition of specimen tip. (c) The detached ignited blob continued to burn whereas the flame of the specimen tip extinguished in the absence of the LPG flame.

AZ91. There was no ignition without some melting. The specimen tip ignition subsequent to melting was governed by the duration of LPG flame exposure. The burning of the specimen tip extinguishing after LPG flame removal. The unignited molten detached blobs ignited when they fell out of the flame. The subsequent burning of the blob was self-sustaining. The target temperatures at which ignition took place for 20 mm diameter specimens followed the sequence: HP Mg > AZ61 > AZ91.

3.6. Mg-Y alloys

Table 5 presents the test results for Mg-1Y and Mg-5Y. The results from *T*-tests using 20 mm specimens suggested similar target temperatures (T_1) at which melting occurred for both alloys. There was no ignition without at least some melting of the specimen tip.

The melting tests for Mg-1Y showed that, following melting, all the specimen tips, except one, remained unignited whereas the detached blobs in all cases ignited. For the specimen tip that did ignite, following melting and detached blob formation, there was smouldering of the specimen tip and the blob, followed by delayed ignition in both. The specimen tip ignited without vigorous burning and the flames extinguished, whereas the detached blob burnt vigorously and burning was self-sustaining.

The melting tests using Mg-5Y showed that, following initial melting, there was only minor ignition even after prolonged exposure (~90 s) to the LPG flame. Fig. 9 presents images of the molten but unignited specimen tip (Specimen 7 in Table 5). Both the specimen tip and the detached blob did not ignite. There was minute ignition in the specimen tip, which readily extinguished even in the presence of the LPG flame. Moreover, the detached blob remained unignited, in contrast to the blobs for HP Mg, AZ61, AZ91 or Mg-1Y.

Out of the five specimen tips for Mg-5Y that melted and formed a detached blob, there was one specimen which ignited following melting, similar to HP Mg, AZ61 and AZ91.

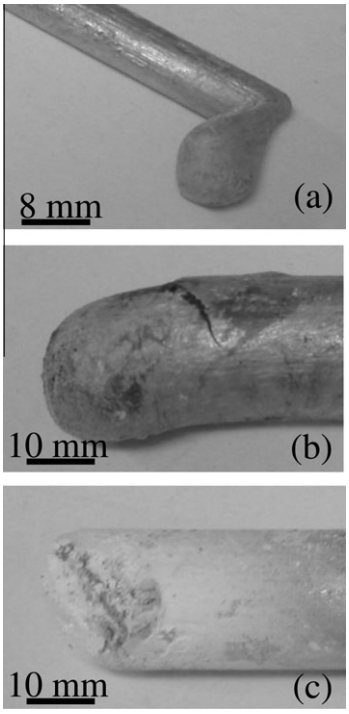

Fig. 8. Effect of LPG flame exposure time on AZ61 and AZ91 specimens: (a) melted but unignited AZ61, 8 mm specimen for which the LPG flame was stopped immediately after specimen tip melting; (b) melted and unignited 20 mm AZ91 specimen; and (c) melted and burnt 20 mm AZ91 specimen.

4. Discussion

4.1. Melting and ignition sequence

The experimental results indicated that melting of the specimen only occurred above a certain T_1. This temperature was alloy dependent and specimen size dependent. The sequence of experiments in Tables 2 and 3 indicated that the T_1 peak temperatures were related to the specimen tip temperatures for the 20 mm specimens. In contrast, all 8 mm specimen tips melted indicating that the target T_1 temperatures were above the T_1 temperature corresponding to specimen tip melting.

After melting, the molten blob either dropped off the specimen tip or remained attached. The detachment of the molten blob depended on the duration of the LPG flame exposure, the alloy and the specimen diameter. The molten blobs tended to detach for AZ61 whereas the molten blobs tended to remain attached for AZ91, possibly due to the larger solidification range for AZ91. The molten blob tended to stay attached to the smaller diameter

Table 5
Flame test results for Mg-Y.

#	Alloy, diameter (mm)	Target T_1 temperature (°C)	Peak T_1 temperature (°C)	Observations	
				Melting	Specimen ignition
1	Mg-1Y, 20	–	595	Yes, detached blob	Yes, delayed ignition
2	Mg-1Y, 20	575	578	No	No
3	Mg-1Y, 20	600	596	Yes, detached blob	No, blob smoulders and ignites
4	Mg-1Y, 20	600	593	Yes, attached blob	No, some smouldering
5	Mg-1Y, 8	–	512	Yes, attached blob	No
6	Mg-1Y, 8	–	526	Yes, detached blob	No, delayed blob ignition
7	Mg-5Y, 20	–	611	Yes, detached blob	No
8	Mg-5Y, 20	600	593	Yes, detached blob	Yes, vigorous; blob unignited
9	Mg-5Y, 20	600	594	Yes, detached blob	No
10	Mg-5Y, 20	580	582	No	No
11	Mg-5Y, 20	580	582	No	No
12	Mg-5Y, 20	550	555	No	No
13	Mg-5Y, 8	600	592	Yes, attached blob	No
14	Mg-5Y, 8	575	579	Yes, attached blob	No

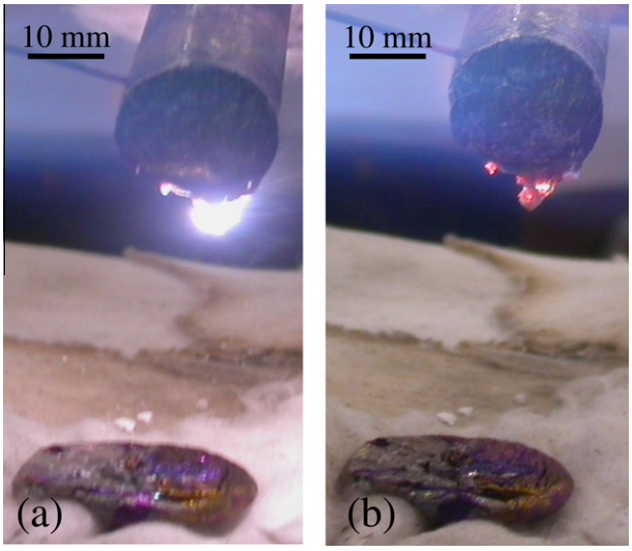

Fig. 9a and b. Images showing the ignition behaviour of a 20 mm Mg-5Y specimen. (a and b) show incipient ignition downgrading to minor oxidation of the melted specimen tip even in the presence of the LPG flame.

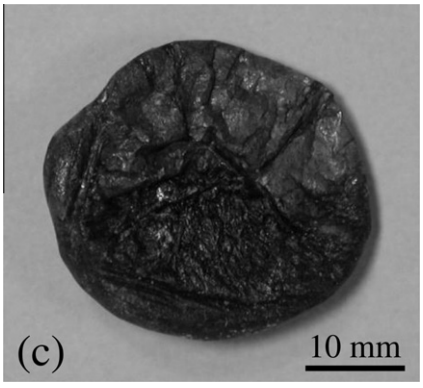

Fig. 9c. Ignition resistance of the blob detached from the 20 mm Mg-5Y specimen shown in Fig. 9(a and b). The blob was mechanically robust and remained unignited.

specimens attributed to the smaller volume of the molten blob as compared to the larger blobs for the 20 mm specimens.

Longer LPG flame exposure led to more melting. However, under no circumstances did ignition take place prior to melting. This was true for all alloys and all specimen diameters. Fig. 7 shows the melting and subsequent ignition sequence for AZ61 compared with that for Mg-5Y in Fig. 9. These figures also show the difference between ignition and flammability. There was initial ignition of the AZ61specimen tip as shown in Fig. 7 and the Mg-5Y specimen tip as shown in Fig. 9. Vigorous flame formation in the AZ61specimen occurred only after ignition kernels were formed (Fig. 7(a) and (b)).There was no vigorous burning of the Mg-5Y specimen even after initial ignition at the specimen tip.

4.2. Specimen tip temperature

Fig. 3(b) shows a schematic of the typical experimental thermal profile. Heat flow was transient, not steady state. Therefore a rigorous estimation of the specimen tip temperature requires transient analysis of the inverse heat conduction problem. However, the tip temperature can be estimated if it is assumed that thermal steady-state was attained at the flame exposed tip at $z = 0$ at time $t = t^*$. The specimen is approximated as a pin-type extended fin whose one end at $z = 0$ is at constant temperature, T. Under assumed steady-state, the temperature distribution within the specimen, characterised by the reduced temperature, θ, is given by [23]:

$$\theta = C_1 \cosh\left(\sqrt{\frac{hP}{kA}}z\right) + C_2 \sinh\left(\sqrt{\frac{hP}{kA}}z\right) \quad (1)$$

where $\theta = T - T_\infty$, T_∞ is the surrounding air temperature, h is the convective heat loss from the specimen to the surrounding air, k is the thermal conductivity of the specimen material, A is the cross-sectional area of the specimen, P is the perimeter of the specimen, and C_1 and C_2 are constants to be determined. This analytical solution assumes that

$$\frac{dT}{dz} = 0 \quad (2)$$

at the unexposed end of the specimen at $z = 200$ mm [23]. This is reasonable since the heat loss through the circular area at the specimen end, at $z = 200$ mm, is much less than the heat loss through the rest of the surface area of the specimen. Solution of Eq. (1) requires estimating C_1, C_2 and the constant m, where m is given by

$$m = \sqrt{\frac{hP}{kA}} \quad (3)$$

Solution of Eq. (1) can be achieved using T_1 and T_2 values at $t = t^*$ at $z = 30$ mm and $z = 195$ mm. Calculation of m requires estimating the convective heat loss from the specimen, given by the Nusselt number, Nu, which was estimated using the empirical relation for fluid cross-flow across an isolated cylinder, given as [23]:

$$Nu = \frac{hD}{k_f} = CRe^n Pr^{(\frac{1}{3})} \quad (4)$$

where k_f is the thermal conductivity of the surrounding air, *Re* is the Reynolds number and *Pr* is the Prandtl number. *C* and *n* are constants, with values of 0.989 and 0.33, respectively for $0.4 < Re < 4$ [23]. The air velocity was assumed to be 0.01 m s^{-1}, and the thermal conductivity of all alloys was assumed the same as that of HP Mg (k = 156 W m^{-1} K^{-1} [24]). (The calculated temperature changed by 0.1 °C with the use of the actual thermal conductivity of AZ61 (80 W m^{-1} K^{-1}) and AZ91 (72 W m^{-1} K^{-1})). The other thermo-physical properties for calculating *Re* were obtained from [23].

Fig. 10 shows the tip temperature at z = 0 for 20 mm specimens, for specimens that underwent some melting and those that did not melt (as observed visually). The data points indicate the average value for the calculated temperature for all specimens of each alloy and are also accompanied by their corresponding error bars. The windows, and the thick black line for Mg-1Y, indicate the freezing range of each alloy. The thin line for HP Mg represents the melting temperature of HP Mg.

The calculated temperatures were in agreement with the melting temperature for HP Mg and the freezing range of the alloys. The calculated tip temperature of the non-melted specimens was lower than that of the specimens with some melting observed visually. Since there was ignition only for the specimens with some melting, these temperature calculations confirm that ignition took place only after at least partial melting.

For Mg-5Y specimens, the calculated tip temperature for the melted specimens showed values higher than that predicted by the phase diagram. In contrast, results for the Mg-1Y specimens showed a melting temperature to be in the range predicted by the phase diagram. This indicates that 5 wt%Y elevated the ignition temperature to somewhat above the melting temperature, whereas a smaller amount of 1 wt%Y did not have any influence on the ignition temperature. This is consistent with the vigorous burning of the detached blobs for Mg-1Y compared with the ignition resistance of detached Mg-5Y blobs (Fig. 9).

In contrast to Fig. 3(a), the TC_2 thermocouple temperature in Fig. 4 did not rise above 30 °C for AZ61 (and the same was also observed for AZ91). This attributed to the lower conductivity of AZ61 (80 W m^{-1} K^{-1}) and AZ91 (72 W m^{-1} K^{-1}) compared with that of HP Mg (156 W m^{-1} K^{-1}).

The data in Tables 2–4 indicated that HP Mg, AZ61 and AZ91ignited only after melting. This result is in agreement with the flame test result of Carapella and Shaw [25]. However, for HP Mg, the results are contrary to the furnace tests of Ravi Kumar et al. [26] and Fassell et al. [11] who reported ignition temperatures lower than the melting temperature. The difference in results for flame tests and the furnace tests is attributed to the temperature gradient in the specimens in the furnace tests. The furnace tests of Ravi Kumar et al. [26] and Fassell et al. [11] had thermocouples embedded within the centre of the specimen. During furnace heating, the specimen was heated from the surface. Thus a temperature gradient is expected within the specimen. The centrally located thermocouple would show a temperature lower than that of the specimen surface.

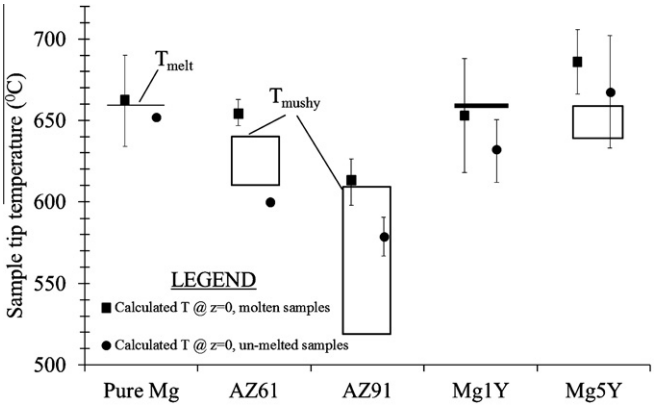

Fig. 10. Estimated sample tip temperature from the pin–fin analysis.

The lack of burning in the current flame experiments can be explained in terms of the competition for oxidation between Mg vapour and the flame engulfing the molten specimen. Since both the fuel vapour from the LPG flame and Mg vapour from the molten alloy require oxygen for reaction, it is reasonable to expect that the limited supply of the oxidant would be distributed between the two competing gaseous species. Vigorous Mg burning would occur only when the oxidation reaction rate of Mg vapour is sufficiently high to form and sustain flames, which in turn would depend upon the Mg vapour availability. Thus, flame tests may result in ignition and delayed burning compared to furnace tests.

4.3. Heat transfer and ignition

Both ignition and vigorous burning are oxidation processes whose rate increases with temperature. Mg oxidation is an exothermic reaction that releases heat, which is proportional to the reaction rate. Thus Mg oxidation at high temperatures releases significantly higher amounts of energy than at lower temperatures. Ignition can be defined as combustion with a reaction rate lower than that of vigorous burning, which is accompanied by flames. Oxidation can take place with solid Mg. Ignition and subsequent vigorous burning is attributed to the availability of Mg vapour. This explains the experimental observation that there was no ignition of any of the Mg alloys when they were solids. Furthermore, the presence of flames indicates combustion involving a gaseous phase. Combustion also depleted the material mass, much like a burning candle, which eventually exhausts the wax. Fig. 1(d) shows the loss of mass in the specimen following burning.

This implies that burning occurred when the oxidation reaction provided sufficient Mg vapour. This depended on the temperature and therefore the heat content to maintain the Mg above its melting temperature. Consider the molten blob, which was either (i) detached and independent of the specimen, or (ii) attached to the specimen tip. In case (i), the detached blob continued to burn whereas the remaining specimen tip continued to burn only as long as the specimen tip was subjected to the LPG flame. This is explained as follows. The heat from burning in the case of the detached blob, minus the heat lost to the surroundings, maintained the blob in a burning state, because the high temperature caused Mg vaporisation from the hot blob. In contrast, the separate specimen tip for case (i) rapidly lost heat (and decreased in temperature) by conduction of heat away from the specimen tip along the length of the specimen, in addition to the heat lost to the surroundings. The higher rate of heat loss for the specimen tip meant that the Mg flame extinguished, unless there was additional heat from the applied LPG flame to maintain the temperature at the specimen tip above the melting temperature, and consequently maintain the combustion via supply of Mg vapour. This situation of higher heat loss was also true for specimens in case (ii) for a specimen tip with a burning tip.

The self-ignition of unignited detached blobs (for pure Mg, AZ61, AZ91 and Mg-1Y) is similarly explained in terms of the heat released during the high temperature oxidation being retained by the blob (minus a small amount of heat lost to the surrounding). As the metal temperature within the oxide crust increased above T_{melt}, the higher volume of the liquid forced the liquid out through

the weakly protective Mg oxide skin. Fresh Mg vapour was exposed to the oxygen in the atmosphere, resulting in ignition and combustion. The oxidation during ignition resulted in more heat release resulting in vigorous burning with flames. The poor mechanical stability of the Mg oxide was also crucial in the burning of the fallen blobs, since a weak oxide crust ruptured relatively easily and allowed the molten metal to spill out and be exposed for vigorous oxidation. Notably, the detached molten blobs of both AZ61 and AZ91 ignited readily. There was likely a contribution due to the presence of low melting temperature eutectics in these alloys that fed the Mg vapours.

Thus, to prevent ignition and burning, the geometry should be such to maintain sufficient heat transfer away from the molten pool to prevent the temperature of the melt staying above T_{melt}. The heat transfer also has to account for the heat release from the oxidation. Thus, while Mg powder or small Mg chips may ignite readily, ignition and burning may be difficult for a large specimen of the same alloy.

4.4. Surface oxide

Fig. 1(d) shows the nature of surface oxide formed for burnt HP Mg whilst Fig. 9(c) shows the surface oxide for Mg-5Y. HP Mg ignited easily, whereas there was delayed ignition for Mg-1Y, and Mg-5Y did not ignite. This is attributed to the surface oxide, thought to contain yttrium-oxide on Mg-5Y. Similar observations were also reported by Fan et al. [27], who found that Y concentrations above 7wt% progressively increased the ignition temperature of Mg. The ignition-proof nature of Y-bearing alloys is attributed to the MgO surface oxide being modified by the presence of Y-oxide. To prevent ignition, enough Y-oxide is needed to completely plug the porous Mg oxide, or to significantly change the properties of the surface oxide. The modification of the Mg oxide in the current experiment was observed in the blue coloured, mechanically stable oxide on Mg-5Y (Fig. 9(c)) compared with the crumbling white MgO residue on the other alloys. The oxide on Mg-1Y was not sufficiently stable to prevent burning. This oxide also was mostly white, and was not as stable as the oxide of Fig. 9(c). Thus, the delayed ignition in Mg-1Y is attributed to molten Mg eventually oozing through the partially covered porous Mg oxide skin.

One Mg-5Y specimen ignited in a manner similar to the specimens of the other alloys. It was visually observed that this Mg-5Y specimen did not have a blue colour as had the other Mg-5Y as-cast specimens. This suggests that this particular specimen did not have enough Y content to form a fully protective oxide skin.

This indicates that there is a critical Y concentration, above which the surface oxide properties change significantly. This is similar to the corrosion properties of Fe–Cr (and Fe–Ni–Cr, Fe–Cr–Ni–Mo–N...) alloys, the basis of stainless steels. In Fe–Cr alloys, the nature of the film formed in aqueous solutions changes from one based on Fe to a film based on Cr (see e.g. [28–36]). This change in film characteristics occurs at about 12 wt%Cr, and concomitantly the corrosion resistance increases by orders of magnitude. The corrosion behaviour is similar to that of Cr, even though there may be only 12 wt% Cr in the alloy. Such abrupt changes in corrosion behaviour (between low corrosion resistance and high corrosion resistance) occur in other systems, such as Co–Cr [37], Ni–Cr [38], Fe–Si [39] and Fe–Ti [40]. Y containing surface films have been also associated with improved corrosion performance for Mg alloys [41–43].

4.5. Limitations

These experiments were specifically aimed at aerospace and auto applications where a component may be exposed directly to a flame. Thus these experiments are different from the prior furnace tests and pouring tests, which focussed on estimating ignition temperatures associated with molten Mg alloys. Whilst the melting temperatures of the samples were calculated (Section 4.2), the ignition temperatures of the alloys was not measured with the present arrangement. Immediate withdrawal of the LPG flame following initial melting resulted in a few ignition kernels on the exposed specimen tips which did not generate enough heat to cause sustained burning. Only extended LPG flame exposure caused ignition and subsequent burning. However, the continuous exposure to a full throttle LPG flame overshadowed any rise in temperature due to the ignition. The heat transfer was also dependent upon the sample thermal conductivity, geometry and size. The experiments were conducted only on cylindrical Mg alloy samples of three different sizes. Moreover, direct measurement of the ignition temperature with the current experimental arrangement would require precise comparison between the actual experiments and the corresponding thermal profile. A further limitation of the current experiment arrangement is that the flame characteristics (such as velocity, chemical and physical structure) were not determined. Hence, the heat transfer from the flame to the sample, and consequently its influence on the flammability were not quantified.

Nevertheless, when ignition did take place after prolonged exposure to the LPG flame, the time to ignition was ~10 s for 20 mm specimens after the initiation of melting. The "time to ignition" and the "time to melting" different by at most 10%. Thus one approach would be to simply use the time to melting as a good estimate of the time to ignition.

Furthermore, within the experimental limitations, there was no burning without melting. Moreover, these experiments indicated that the concept of an ignition temperature may be of limited use for a Mg structure exposed to a flame, provided that there is a significant possibility of heat conduction away from the specimen tip. In contrast, for situations when there is no significant conduction of heat from the specimen tip, then the blob experiments may provide a good indication of behaviour. Namely there was ignition and complete burning for HP Mg, AZ61 and AZ91, whereas Mg-5Y resisted ignition and burning.

Time to melting (as a measure of time to ignition) is clearly geometry dependent and was not measured in the present research. Time to melting depends on the flame characteristics (and particularly the heat input into the specimen), the LPG flame-specimen arrangement (and particularly if the specimen is horizontal or vertical) and the specimen geometry (and in particular the heat extraction from the specimen tip). A vertical specimen in a horizontal flame appears to be more complicated than the present arrangement of a horizontal LPG flame impinging onto the specimen tip of a horizontal specimen. A vertical specimen, with the specimen tip (in the LPG flame) at the bottom of the specimen, has the complication that the heat input to the specimen would include a large contribution from the specimen flame, once the specimen burns. There would be the complication that the molten material from the specimen tip would flow along the specimen for a vertical specimen, with the specimen tip (in the LPG flame) at the top of the specimen.

For the present arrangement of a horizontal LPG flame impinging onto the specimen tip of a horizontal specimen, some thought could be given to a standardisation along the following lines. The time to melting could be normalised by the heat input into the specimen tip by the LPG flame and also by the heat conduction away from the specimen tip. This would require more detailed modelling to extend the modelling outlined in Section 4.2. It might be possible to use a combination of modelling and experimental measurement to assess the amount of heat input into the specimen. The heat conduction away from the specimen tip could be estimated by building on the modelling of Section 4.2 to establish

a detailed transient model. Such standardisation would need to be verified by experiments measuring the time to melting for various flames, specimen geometries, variable convective heat loss and material type.

5. Conclusions

1. There were important differences in the ignition characteristic for HP Mg, AZ61 and AZ91 of (i) the cylindrical Mg specimens subjected to direct LPG flame impingement and (ii) a detached blob of molten metal from the specimen tip.
2. The cylindrical specimen tips required direct continued exposure of the LPG flame to ignite and extinguished once the LPG flame was withdrawn.
3. The detached unignited molten blob, from the specimen tip, ignited readily even without the exposure to the LPG flame. Burning was self-sustaining for HP Mg, AZ61 and AZ91 blobs.
4. Detached blobs of Mg-5Y did not burn.
5. Mg-5Y specimens showed good resistance to ignition. There was no ignition even after prolonged exposure to the LPG flame.
6. The cylindrical specimens provide insight into the flammability of Mg structures, where there is significant possibility of heat conduction away from the specimen tip exposed to the flame.
7. For situations when there is no significant conduction of heat from the specimen tip, then the blob experiments may provide a good indication of behaviour for molten material. Namely there was ignition and complete burning for HP Mg, AZ61 and AZ91, whereas Mg-5Y resisted ignition and burning.
8. The flammability resistance of Mg-5Y is attributed to a more protective surface oxide on the molten alloy.
9. Time to melting and time to ignition depend on the characteristics of the applied flame (and particularly the heat input into the specimen), the flame-specimen arrangement (and particularly if the specimen is horizontal or vertical) and the specimen geometry (and in particular the heat extraction from the specimen tip).

Acknowledgements

The research on Mg flammability, corrosion and stress corrosion cracking is supported by Boeing Research and Technology, CAST CRC, the Australian Research Council Centre of Excellence Design of Light Alloys, and GM Global Research and Development. CAST CRC was established under, and is funded in part by the Australian Federal Government's Cooperative Research Centre scheme. The authors would also like to thank Mr. Xuewen Yuan for his assistance in performing the experiments.

References

[1] A. Atrens, M. Liu, N.I.Z. Abidin, Corrosion mechanism applicable to biodegradable magnesium implants, Materials Science and Engineering B, 2010, doi:10.1016/j.mseb.2010.12.017.
[2] G.L. Song, A. Atrens, Corrosion mechanisms of magnesium alloys, Advanced Engineering Materials 1 (1999) 11–33.
[3] G.L. Song, A. Atrens, Understanding magnesium corrosion: a framework of improved alloy performance, Advanced Engineering Materials 5 (2003) 837–858.
[4] N. Winzer, A. Atrens, G.L. Song, E. Ghali, W. Dietzel, K.U. Kainer, N. Hort, C. Blawert, A critical review of the stress corrosion cracking of magnesium alloys, Advanced Engineering Materials 7 (2005) 659–693.
[5] G. Foerster, HiLoN: a new approach to magnesium die casting, Advanced Materials and Processes 154 (1998) 79–81.
[6] Z. Chen, X. Ren, Y. Zhang, Effect of RE on the ignition proof, microstructure and properties of AZ91D magnesium alloy, Journal of Institute of Science and Technology (Beijing) 12 (2005) 540–544.
[7] R. Jin-song, L. Hua-ji, X. Han-song, Ignition-proof mechanism of ZM5 magnesium alloy added with rare earth, Journal of Central South University Technology 17 (2010) 28–33.
[8] M. Sakamoto, S. Akiyama, K. Ogi, Suppression of ignition and burning of molten Mg alloys by Ca bearing stable oxide film, Journal of Materials Science Letters 16 (1997) 1048–1050.
[9] Z. Xiaoqin, W. Qudong, L. Yizhen, D. Wenjiang, C. Lu, Z. Yanping, C.Q. Zhai, X.P. Xu, Study of ignition proof magnesium alloy with beryllium and rare earth additions, Scripta Materialia 43 (2000) 403–409.
[10] Z. Xiaoqin, W. Qudong, L. Yizhen, Z. Yanping, D. Wenjiang, Z. Yunhu, Influence of beryllium and rare earth additions on ignition proof magnesium alloys, Journal of Materials Processing Technology 112 (2001) 17–23.
[11] W.M. Fassell, L.B. Gulbransen, J.R. Lewis, J.H. Hamilton, Ignition temperatures of magnesium and magnesium alloys, Journal of Metals (1951) 522–528.
[12] W. Li, H. Zhou, W. Zhou, W.P. Li, M.X. Wang, Effect of cooling rate on ignition point of AZ91D–0.98wt%Ce magnesium alloy, Materials Letters 61 (2007) 2772–2774.
[13] X. Huang, H. Zhou, Z. He, Analysis on ignition-proof mechanics of AZ91D alloy added with Ce, Journal of Materials Science and Technology 18 (2002) 279–280.
[14] P.-Y. Lin, H. Zhou, W. Li, W.-P. Li, N. Sun, R. Yang, Interactive effect of cerium and aluminium on the ignition point and the oxidation resistance of magnesium alloy, Corrosion Science 50 (2008) 2669–2675.
[15] P.-Y. Lin, H. Zhou, N. Sun, W.-P. Li, C.-T. Wang, M.-X. Wang, Q.-C. Guo, W. Li, Influence of cerium addition on the resistance to oxidation of AM50 alloy prepared by rapid solidification, Corrosion Science 52 (2010) 416–421.
[16] J.F. Fan, G.C. Yang, S.L. Chen, H. Xie, M. Wang, Y.H. Zhou, Effects of rare earth (Y, Ce) additions on the ignition points of magnesium alloys, Journal of Materials Science 39 (2004) 6375–6377.
[17] T.-S. Shih, J.-H. Wang, K.-Z. Chong, Combustion of magnesium alloys in air, Materials Chemistry and Physics 85 (2004) 302–309.
[18] B.-S. You, M.-H. Kim, W.-W. Park, I.-S. Chung, Effects of Al and Y additions on the oxidation behaviour of Mg–Ca base molten alloys, Materials Science Forum 419–422 (2003) 581–586.
[19] B.-H. Choi, I.-M. Park, B.-S. You, W.-W. Park, Effects of Ca and Be additions on high temperature oxidation behaviour of AZ91 alloys, Materials Science Forum 419–422 (2003) 639–644.
[20] Y.-B. Huang, B.-S. You, B.-H. Choi, W.-W. Park, I.-S. Chung, S.K. Suh, Model for the protective oxidation of Mg–Ca alloys containing Be at elevated temperature, Materials Science Forum 449–452 (2004) 637–640.
[21] H. Eyring, B.J. Zwolinski, The critical temperature for combustion of metals and their alloys, in: Record of Chemical Progress, Wayne University, 1947.
[22] M. Liu, D.S. Shih, C. Parish, A. Atrens, The ignition temperature of Mg alloys WE43, AZ31 and AZ91, Corrosion Science 54C (2012) 139–142.
[23] W.S. Janna, Engineering Heat Transfer, second ed., CRC Press, 2000.
[24] F.P. Incropera, D.P. Dewitt, Introduction to Heat Transfer, third ed., John Wiley and Sons, 1996.
[25] L.A. Carapella, W.E. Shaw, Do solid magnesium alloys burn?, Metals and Alloys 22 (1945) 415–416
[26] N.V. Ravi Kumar, J.J. Blandin, M. Suery, E. Grosjean, Effect of alloying elements on the ignition resistance of magnesium alloys, Scripta Materialia 49 (2003) 225–230.
[27] J.F. Fan, C.L. Yang, G. Hana, S. Fanga, W.D. Yanga, B.S. Xu, Oxidation behavior of ignition-proof magnesium alloys with rare earth addition, Journal of Alloys and Compounds 509 (2011) 2137–2142.
[28] P. Bruesch, K. Muller, A. Atrens, H. Neff, Corrosion of stainless steels in chloride solution: an XPS investigation of passive films, Applied Physics A 38 (1985) 1–18.
[29] S. Jin, A. Atrens, ESCA studies of the structure, composition of the passive film formed on stainless steels by various immersion times in 0.1 M NaCl solution, Applied Physics A 42 (1987) 149–165.
[30] S. Jin, A. Atrens, Passive films on stainless steels in aqueous media, Applied Physics A 50 (1990) 287–300.
[31] M.A. Streicher, Corrosion of stainless steels in boiling acids and its suppression by ferric salts, Corrosion 14 (1958) 59t–70t.
[32] T.N. Rhodin, The relation of thin films to corrosion, Corrosion 11 (1956) 465t–475t.
[33] M.A. Streicher, The role of carbon, nitrogen, and heat treatment in the dissolution of iron–chromium alloys in acids, Corrosion 29 (1973) 337–360.
[34] I. Olefjord, B.-O. Elfstrom, The composition of the surface during passivation of stainless steels, Corrosion 38 (1982) 47–52.
[35] K. Sugimoto, S. Matsuda, Passive and transpassive films on Fe–Cr alloys in acid and neutral solutions, Materials Science and Engineering 42 (1980) 181–189.
[36] G. Okamoto, Passive films of 18–8 stainless steel structure and its function, Corrosion Science 13 (1973) 471–489.
[37] A.S. Lim, A. Atrens, ESCA studies of Cr–Co alloys, Applied Physics A 54 (1992) 270–278.
[38] A.S. Lim, A. Atrens, ESCA studies of Ni–Cr alloys, Applied Physics A 54 (1992) 343–349.
[39] A.S. Lim, A. Atrens, ESCA studies of Si–Fe alloys, Applied Physics A 53 (1991) 273–281.
[40] A.S. Lim, A. Atrens, ESCA studies of Si–Fe alloys, Applied Physics A 54 (1992) 500–507.
[41] M. Liu, P. Schmutz, P.J. Uggowitzer, G. Song, A. Atrens, Influence of yttrium (Y) on the corrosion of Mg-Y binary alloys, Corrosion Science 52 (2010) 3687–3701.
[42] H.B. Yao, Y. Li, A.T.S. Wee, Corrosion behaviour of melt-spun $Mg_{65}Ni_{20}Nd_{15}$ and $Mg_{65}Cu_{25}Y_{10}$ metallic glasses, Electrochimica Acta 48 (2003) 2641–2650.
[43] H.B. Yao, Y. Li, A.T.S. Wee, J.S. Pan, J.W. Chai, Effect of Y addition on the corrosion behaviour of melt-spun amorphous Mg–Cu ribbons, Electrochimica Acta 8 (2001) 575–580.